# Middle East Technical University
# Department of Electrical and Electronics Engineering

## EE568 - Selected Topics on Electrical Machines
### Spring 2019 – 2020

## Project #4: Analysis of a Five-Phase Axial Flux PMSM
**June 28th, 2020**

### Introduction

In this project, the design of a five-phase axial-flux permanent magnet synchronous machine with a novel winding topology will be investigated. As discussed previously, this is an already designed and prototyped machine. Therefore, even if the main electric machine sizing and design procedure will be followed, some parameters are already known and they will only be verified. After the analytical analysis part, the results will be justified using FEA. The discrepancies between the analytical model and the finite element model will be discussed. Following this, several changes on the model will be performed (such as changing the magnet thickness and airgap), to investigate whether first iteration is optimal or not. Finally, the report will be concluded with an overall discussion of the design, including both advantages and drawbacks of this topology.

### Analytical Calculation

A machine, similar and three-phase version of this one is already designed, prototyped and tested by Gökhan Çakal. The only modification to Gökhan's version is increase in the number of phases, which is five. Resultantly, the dimensions and electrical parameters of the machine are already known and will be verified in this part of the report.

The machine specifications can be summarized as:

- Rated power: 1.6 kW
- Rated phase current: 22 Arms
- Rated torque: 30 Nm
- Electrical synchronous frequency: 35 Hz
- Winding is formed of flat aluminum wires, arranged as 60 loops of 4 sides
- Number of phases: 5
- Number of poles: 8

## 1. Magnetic Loading of the Machine

Calculation of the magnetic loading of the machine requires several design variables. These can be summarized as follows:

- Magnet thickness ($l_m$): 12 mm
- Stator thickness ($l_s$): 11 mm
- Airgap thickness ($l_g$): 2.5 mm
- Magnet grade: N38H
- $B_r$ (at 80$^o$C): 1.22 T
- $H_c$ (at 80$^o$C): 924.6 kA/m
- $\mu_r$: 1.05
- Saturation point of electrical steel: 1.5 T

Considering the topology of the machine, magnetic equivalent circuit can be derived as in Fig. 1.

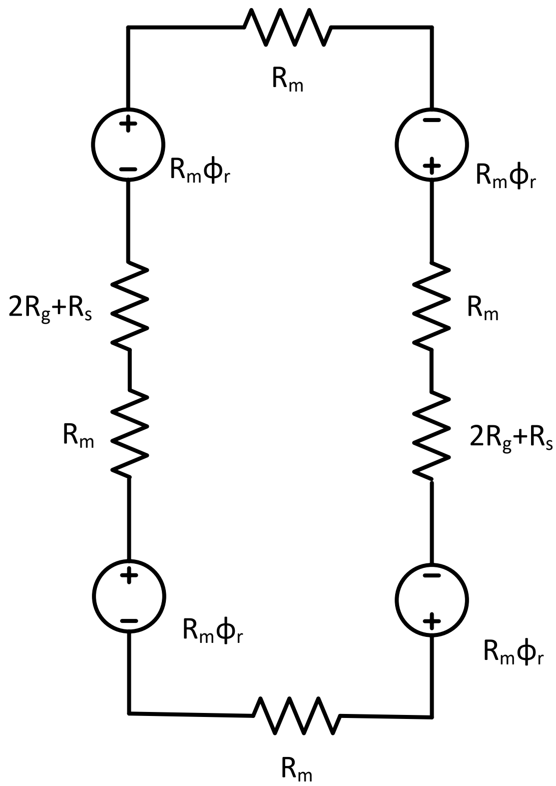


*Figure 1: Magnetic Equivalent Circuit*

Here, as the relative permeability of the electrical steel is too large, $R_r$ can be ignored. Also, flux leakage paths between two magnets are long, therefore leakage reluctance can also be ignored. Using remaining circuit elements, we can obtain air-gap flux density as given below.

$$4R_m\phi_r = \phi_g(4R_m + 2R_s + 4R_g)$$

$$R_m B_r = B_g\left(R_m + \frac{1}{2}R_s + R_g\right)$$

$$\frac{l_m}{\mu_r}B_r = \left(\frac{l_m}{\mu_r} + \frac{l_s}{2} + l_g\right)B_g$$

$$B_g = \frac{B_r\left(\frac{l_m}{\mu_r}\right)}{\frac{l_m}{\mu_r} + \frac{l_s}{2} + l_g} = 0.718\ T$$

This value is the peak flux density over a pole area, assuming square-wave-shaped flux density distribution. To find the magnetic loading, the magnitude of the fundamental component of this square wave should be calculated.

$$\hat{B}_{g,1} = \frac{4}{\pi}0.718 = 0.914\ T$$

## 2. Electric Loading of the Machine

In axial flux machines calculation of electric loading is different from radial flux machines. As the whole stator surface coincides with the airgap, linear current density value can change as a function of radius. In [1], linear current density is calculated on the inner radius, which is the maximum linear current density in the motor. In the current topology, each corner of each "loop" on each layer can be considered as a turn in a slot. Therefore, resultant total turn number becomes 240. Following this approach, electric loading of the machine can be calculated as follows:

$$\widehat{A_{in}} = \frac{N\hat{I}}{\pi D_i} = \frac{240 \times 30}{\pi \times \ 124 \times 10^{-3}} = 18483\,\frac{A}{m}$$

## 3. Verification of Torque Equation

Torque equation for an electric machine is:

$$T = \frac{1}{2}\widehat{A_{in}}\widehat{B_{\delta 1}} r_{in} S_{rot}$$

where S is rotor surface area, and $r_{in}$ is rotor inner diameter. Parameters is the torque equation are:

- Â = 18483 A/m
- $\hat{B}$ = 0.914 T
- $r_{in} = 0.062\ m$
- $S_{rot} = \pi(r_{out}^2 - r_{in}^2) = 0.0586\ m^2$

Using the values given, output torque of the motor is calculated as 30.7 Nm, as expected.

## 4. Back EMF Calculation and Verification of Power Equation

To verify the power of the machine using both mechanical and electrical parameters, the back EMF of the machine should be known. The power equality that should be satisfied is:

$$P = T\ \omega = 5\,\frac{\widehat{E_{ph}}\widehat{I_{ph}}}{2}$$

Phase back EMF can be calculated using previously obtained parameters.

$$\widehat{E_{ph}} = 2\pi f\ k_{w1}\ N_{ph} B_{avg} A_{pole}$$

$$\widehat{E_{ph}} = 2\pi \times 35 \times 0.982 \times 24 \times \frac{2}{\pi} 0.914 \times \frac{0.0586}{8} = 22\ V$$

As a result,

$$P = 5\frac{22 \times 30}{2} = 1650\ W$$
$$P = 30.7 \times 2\pi \times 8.75 = 1687\ W$$

Power equality is satisfied. Therefore, verified machine specifications can be summarized as given below:

- Output torque: 30.7 Nm
- Shaft speed: 8.75 Hz
- Number of poles: 8
- Number of phases: 5
- Phase back EMF: 15.6 V
- Phase current: 21.2 A
- Axial length: 80 mm
- Inner radius: 62 mm
- Outer radius: 150 mm
- Air-gap length: 2.5 mm (each)
- Stator length: 11 mm
- Magnet thickness: 12 mm
- Number of loops: 60, (24 series turns per phase)

## FEA Results

The motor is modelled and analyzed using FEA. Phase back EMF, airgap flux density distribution and output torque graphs are given in Fig. 2-4.

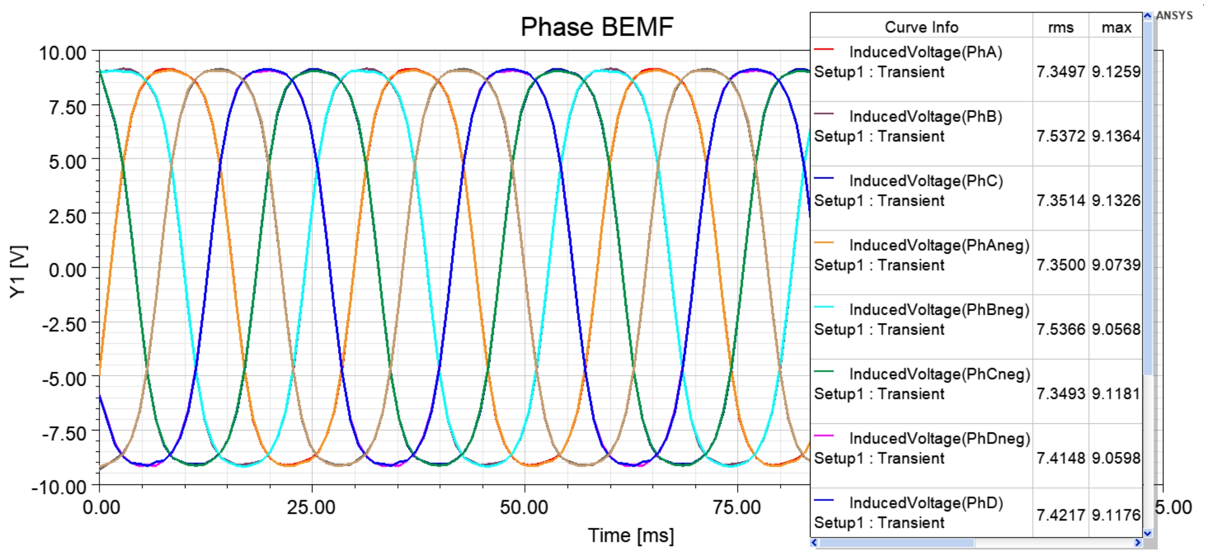


*Figure 2: Phase Back EMF*

In electrical point of view, the machine has five phases. However mechanically, it is formed of 10 groups of 6 winding loops. In Maxwell, the machine windings have also been defined in this manner. As a result, in the analysis results, back EMF are half of the nominal value, i.e. it actually provides us a voltage waveform with a peak of 18 V.

Both the back EMF and airgap flux density values are lower than the expected and analytically calculated ones. The main reason for that is the leakage fluxes are ignored in analytical models. As the machine is air-cored, air crossing of the main flux path is long and leakage flux paths have also some significant length compared to main flux paths. This leakage result in a lower airgap flux density, phase back EMF and torque.

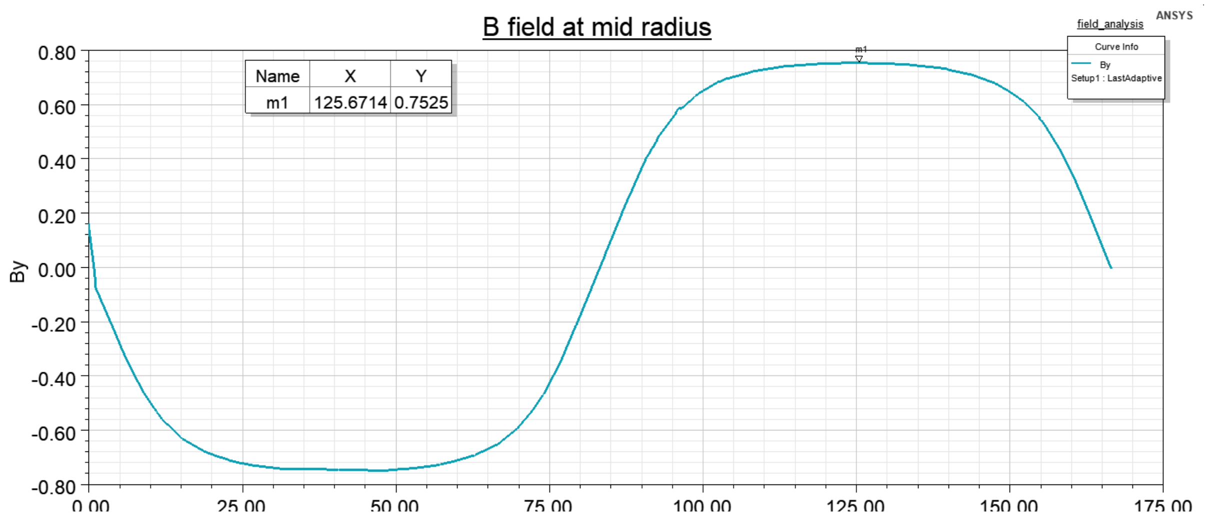


*Figure 3: Airgap B Distribution*

Phase resistance is calculated using copper loss calculation of Maxwell. In this model, the machine has five-phases which are excited with 20 A peak current. With a simple calculation, phase resistance is found as 60 mΩ. This result is legitimate, as in Gökhan's prototype, which had 10 series turns in each phase, phase resistance was 100 mΩ. The result is given in Fig. 5, below.

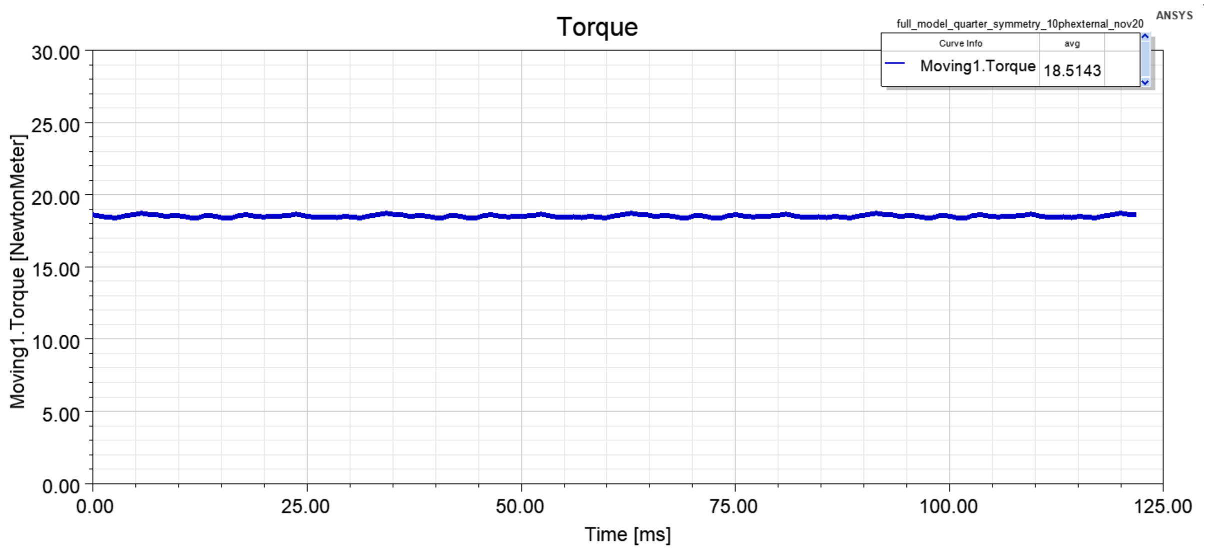


*Figure 4: Output Torque*

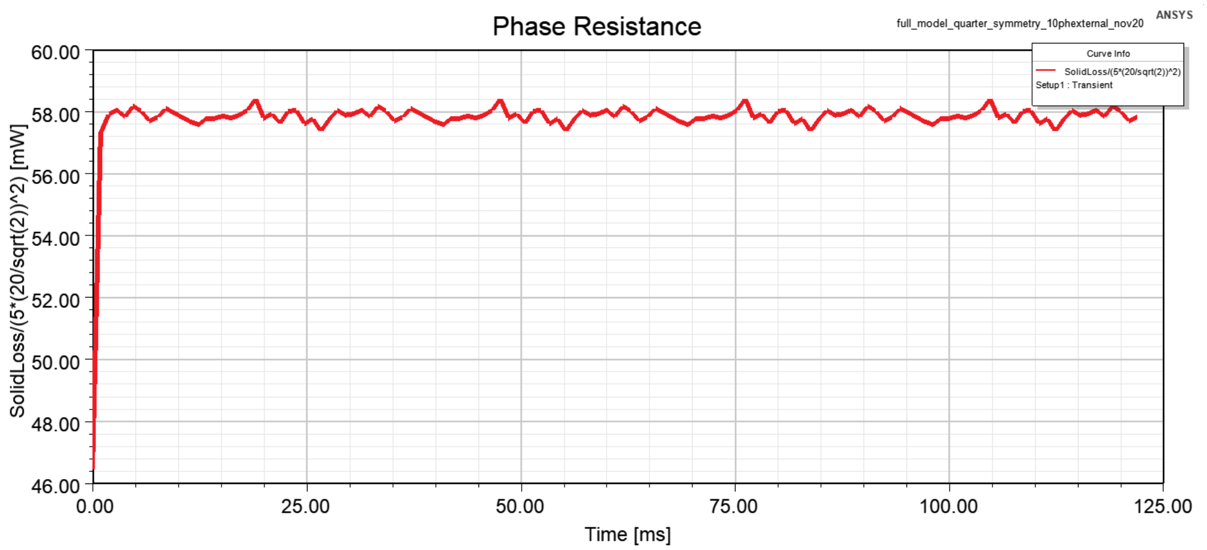


*Figure 5: Phase Resistance*

Phase inductance of the machine is tabulated in Table 1. The machine has quite low inductances, which is expected for an air-cored machine.

Low phase inductance can be disadvantageous. Because of low electrical time constant of the winding, high switching frequency and faster control loop should be adapted. By means of fault tolerance, low inductance is unwanted since high inductance provides lower short circuit currents.

*Table 1: Inductance Matrix of the Motor (x1e-6 H)*

| | A | B | C | D | E |
|---|---|---|---|---|---|
| A | 44.2 | 7.55 | -25.2 | -25 | 7.78 |
| B | 7.54 | 44.1 | 7.6 | -24.9 | -24.9 |
| C | -25.2 | 7.61 | 44.1 | 7.73 | -25.1 |
| D | -25 | -24.9 | 7.73 | 44.1 | 7.48 |
| E | 7.78 | -24.9 | -25.1 | 7.48 | 44.1 |

At this operating point, the efficiency is also calculated in Maxwell. Efficiency plot as a function of time is given in Fig. 6, below. It is found as 97.6% which is unexpectedly high. I would expect lower efficiency because of copper losses in the machine.

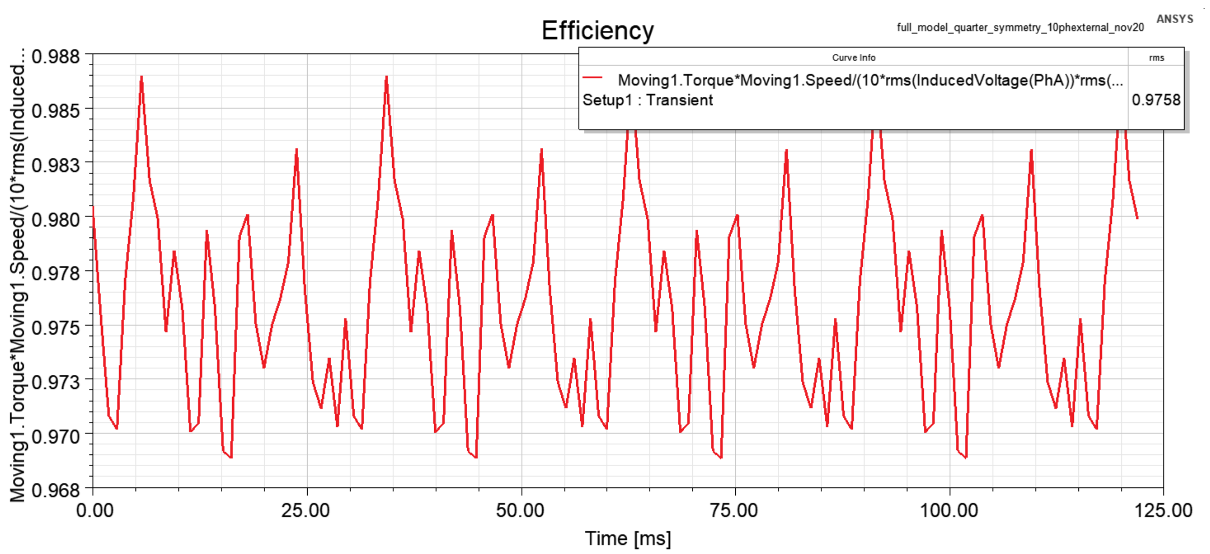


*Figure 6: Efficiency of the Motor*

## Alternative Designs

Two alternative models have also been analyzed in order to compare to the initial design. In these designs, airgap is decreased from 2.5 to 1 mm, and magnet thickness is decreased from 12 to 8 mm, respectively.

Induced back EMF and torque waveforms of the design with smaller airgap are given in Fig. 7-8.

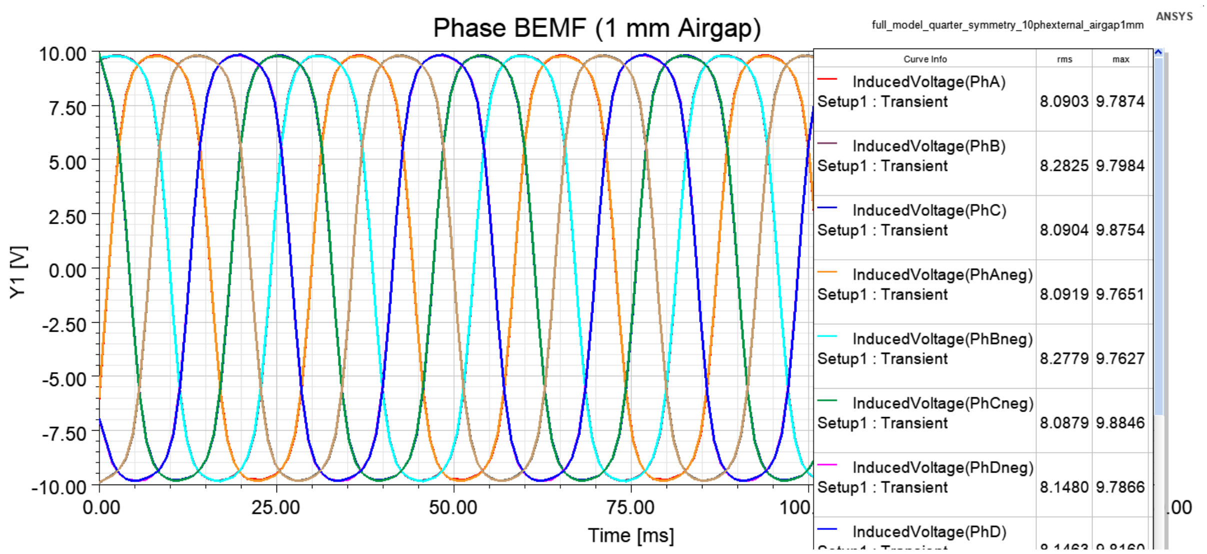


*Figure 7: Induced Back EMF of the Design With 1 mm Airgap*

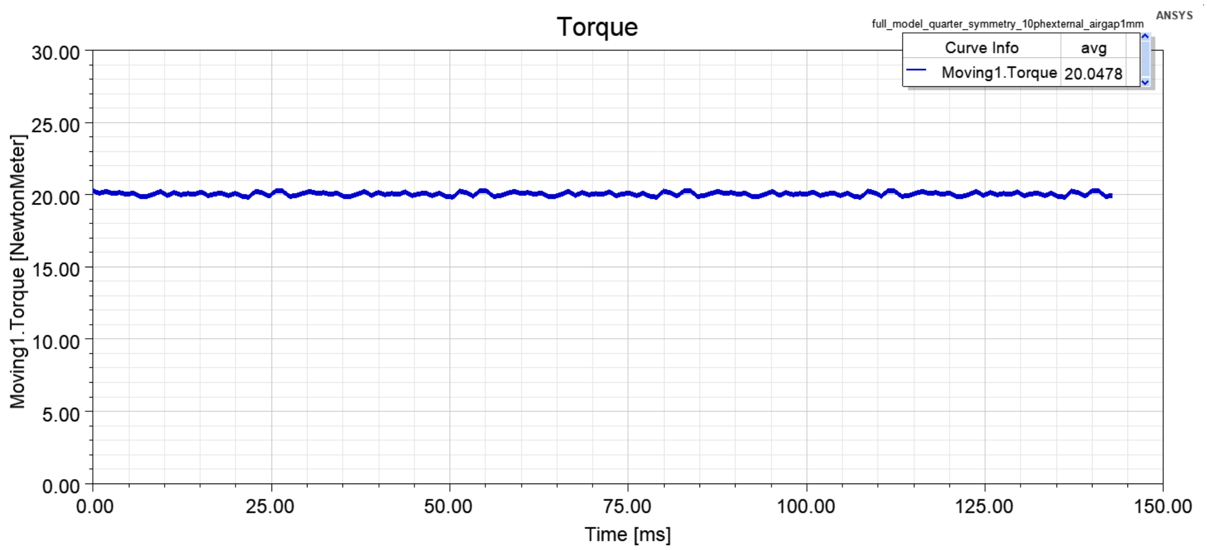


*Figure 8: Torque of the Design With 1 mm Airgap*

In this design, both induced voltage and torque have been improved as expected, but these improvements are around 10%, where the airgap is decreased by 60% and decreased to a mechanically problematic level. The stator of the machine is hand-crafted and the windings have been covered with epoxy. Stator of the machine may not have an even and smooth surface. 1 mm airgap is too small for a possible manufacturing tolerance. Therefore, in this trade-off, decreasing the airgap further is not a wise option. As the machine is air-cored, equivalent airgap is already too large and further improvements do not affect the output performance of the machine.

Induced back EMF and torque waveforms of the design with smaller airgap are given in Fig. 9-10.

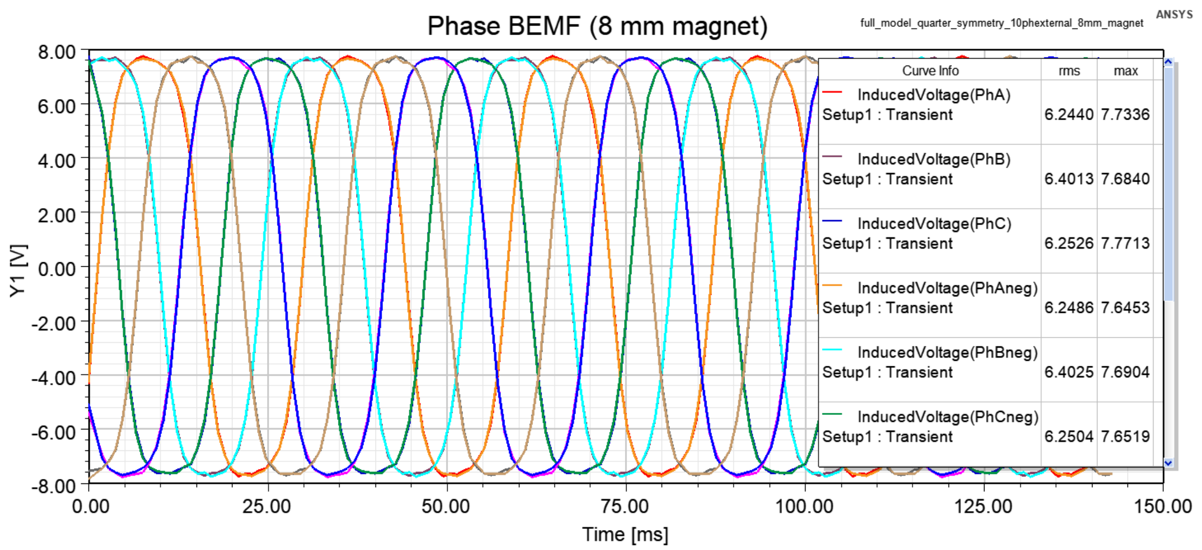


*Figure 9: Induced Back EMF of the Design With 8 mm Magnet*

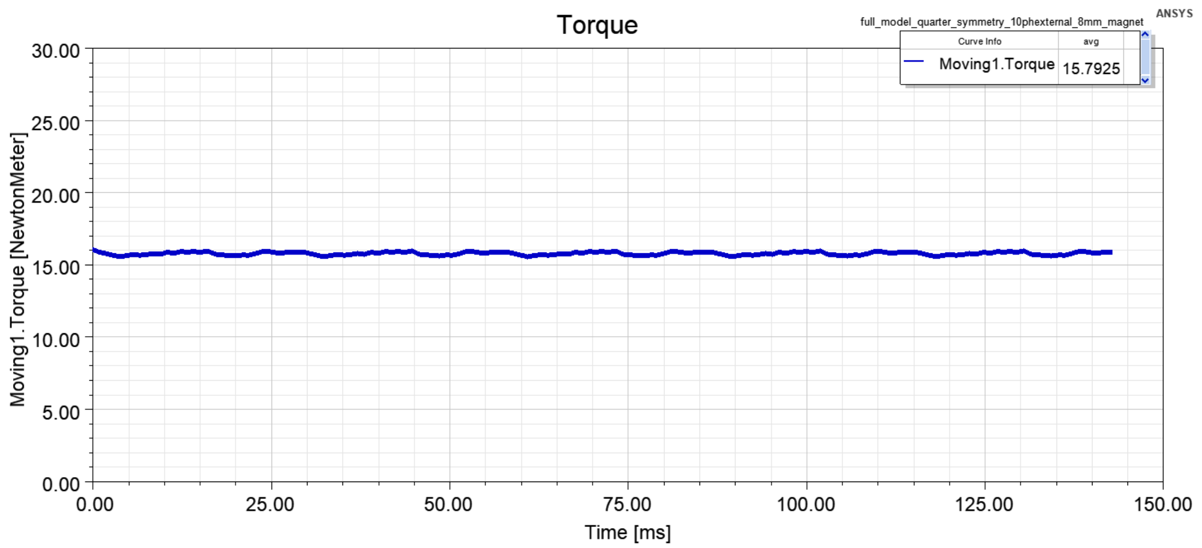


*Figure 10: Torque of the Design With 8 mm Magnet*

Thinner magnets have improved the performance of the magnets significantly, as expected. Magnet weight and cost is decreased by 33%, where back EMF and output torque are decreased around

16%. If one of the major design constraints becomes cost, the magnets of the motor can be thinner and outer radius of the motor can be slightly increased to keep the rated torque.

To manufacture a prototype of this machine, the material consumption becomes:

- Magnet: 4.8 kg
- Aluminum: ~5 kg
- Steel: 18.4 kg
- Epoxy resin: 2.8 kg
- Total mass: 31 kg
- Total volume: 4.69 L
- Volumetric power density: 0.341 kW/L
- Gravimetric power density: 0.052 kW/kg
- Volumetric torque density: 6.4 Nm/L
- Gravimetric torque density: 0.968 Nm/kg

## Discussion and Conclusion

In this project, the design of a five-phase axial flux air-cored permanent magnet synchronous machine is described and verified using both analytical and numerical methods. Several modifications on the initial design have also been considered.

The major advantage of this machine is ease of manufacturability (especially for mass production). However, power and torque density of the machine is quite low, which is mainly a result of air-cored topology. One other drawback of air-cored machines is high magnet cost. Almost 5 kg of magnets produce only 1.6 kW output power, which is inefficient. On the other hand, core loss is minimized since there is no steel in the stator. This design is a better solution for the applications where high power and torque density are not required, but high torque and low speed characteristics are expected.

## References

[1] A. Parviainen, "Design of axial-flux permanent-magnet low-speed machines and performance comparison between radial-flux and axial-flux machines," Ph.D. dissertation, Lappeenranta University of Technology, Lappeenranta, Finland, 2005. Accessible online.